

International Conference on Space Optics—ICSO 2004

Toulouse, France

30 March–2 April 2004

Edited by Josiane Costeraste and Errico Armandillo



Ozone monitoring instrument flight-model on-ground and inflight calibration

*Marcel Dobber, Ruud Dirksen, Pieternel F. Levelt,
Gijsbertus van den Oord, et al.*



OZONE MONITORING INSTRUMENT FLIGHT-MODEL ON-GROUND AND IN-FLIGHT CALIBRATION

Marcel Dobber⁽¹⁾, Ruud Dirksen^(1,2), Pieter F. Levelt⁽¹⁾, Gijsbertus van den Oord⁽¹⁾, Glen Jaross⁽³⁾, Matt Kowalewski⁽³⁾, George H. Mount⁽⁴⁾, Donald Heath⁽⁵⁾, Ernest Hilsenrath⁽⁶⁾, Richard Cebula⁽³⁾

⁽¹⁾Royal Netherlands Meteorological Institute (KNMI), PO Box 201, 3730 AE De Bilt, NL, dobber@knmi.nl, levelt@knmi.nl, oordvd@knmi.nl

⁽²⁾Space Research Organisation Netherlands (SRON), Sorbonnelaan 2, 3584 CA Utrecht, NL, dirksen@knmi.nl

⁽³⁾Science systems & Applications Inc, GSFC-Code 916, Greenbelt, MD USA 20771, jaross@qhearts.gsfc.nasa.gov, mattk@ventus.gsfc.nasa.gov, richard_cebula@ssaihq.com

⁽⁴⁾Dept. of Civil and Env. Engineering, Washington State University, Pullman, WA USA 99164, gmount@wsu.edu

⁽⁵⁾Research Support Instruments Inc, 5735 Arapahoe Ave., suite 2A, Boulder, CO USA 80303, d.f.heath@worldnet.att.net

⁽⁶⁾Atm. Chemistry and Dynamics branch, GSFC-code 916, Greenbelt, MD USA 20771, ernest.hilsenrath@nasa.gov

ABSTRACT

The Ozone Monitoring Instrument (OMI) is an ultraviolet-visible imaging spectrograph that uses two-dimensional CCD detectors to register both the spectrum and the swath perpendicular to the flight direction. This allows having a 114 degrees wide swath combined with an unprecedented small ground pixel (nominally 13 x 24 km²), which in turn enables global daily ground coverage with high spatial resolution. The OMI instrument is part of NASA's EOS-AURA satellite, which will be launched in the second half of 2004. The on-ground calibration of the instrument was performed in 2002. This paper presents and discusses results for a number of selected topics from the on-ground calibration: the radiometric calibration, the spectral calibration and spectral slit function calibration. A new method for accurately calibrating spectral slit functions, based on an echelle grating optical stimulus, is discussed. The in-flight calibration and trend monitoring approach and facilities are discussed.

Keywords: calibration, remote sensing, ultraviolet-visible, imaging spectrograph.

1. INTRODUCTION

The primary objective of the OMI instrument on the EOS-AURA satellite is to obtain daily global measurements of ozone and nitrogen dioxide in both the troposphere and stratosphere and tropospheric aerosols. The recovery of the ozone layer, the depletion of ozone at the poles, tropospheric pollution and climate change are the central science issues addressed by the OMI mission.

The atmospheric constituent concentrations are retrieved from nadir observations of backscattered light from the sun on the earth's atmosphere in the ultraviolet-visible wavelength range (270-500 nm). Both Differential Optical Absorption Spectroscopy (DOAS) and algorithms that have been developed for the TOMS instrument series for the retrieval of total columns of the various atmospheric constituent concentrations are used. The ozone profile is

obtained from strong wavelength dependence of the absorption cross-section between 270 and 330 nm.

OMI combines a high spatial resolution and daily global coverage. In this way tropospheric constituents can be observed with high spatial resolution and cloud-free ground pixels are more easily obtained as compared to instruments with scanning mirrors, such as GOME and SCIAMACHY. This is important to enable OMI to monitor tropospheric pollution phenomena, like biomass burning and industrial pollution, on a regional scale. Monitoring tropospheric pollution is essential for studying human impact on the earth's atmosphere and climate.

OMI-EOS will deliver absolutely calibrated spectral radiances and irradiances from 270 to 500 nm. These are used to retrieve the primary data products: ozone total column, ozone vertical profile, UV-B flux, nitrogen dioxide total column, aerosol optical thickness, cloud effective cover, cloud top pressure and secondary data products: total column SO₂, BrO, HCHO and OCIO.

OMI has been developed by Dutch and Finnish industry under contract with the Netherlands Agency for Aerospace Programmes (NIVR) and the Finnish Meteorological Institute (FMI). The Royal Netherlands Meteorological Institute (KNMI) is the Principal Investigator institute for the OMI instrument. The international OMI science team has approximately 60 members.

For OMI, and remote sensing instruments like OMI, a good on-ground calibration delivering reliable calibration key data for use in the 0-1 data processing is essential to meet the mission objectives, especially when the data is to be compared to and to become part of long-term ozone trend recordings. In order to keep and maintain a good calibration status of the instrument after launch, a considerable in-flight effort is required. For an instrument such as OMI this is only possible when automated processing facilities for in-flight calibration and trend monitoring are developed, because of the high data rates and complexity of the instrument.

The results of the on-ground calibration and the approach and facilities for in-flight calibration are the subjects of this paper.

2. OMI INSTRUMENT DESCRIPTION

The OMI instrument is a compact nadir viewing ultraviolet-visible imaging spectrograph with two spectral channels, each having a two-dimensional frame transfer CCD. The 114 degrees large field-of-view (FOV) perpendicular to the flight direction yields a 2600 km wide swath that is large enough to achieve global daily coverage of the earth's atmosphere. The swath is sampled by 60 (electronically binned) ground pixels; the size of a pixel projected on the earth's surface is 13x24 km² (flight direction x swath direction) in the nadir direction. The pixels close to the edge of the swath become progressively larger. By employing a two-dimensional CCD the spectrum of every ground pixel is recorded simultaneously. In one dimension of the CCD the spectrum is recorded while the viewing direction is recorded in the other dimension. The operational temperature of the optical bench is 265 K and the temperature of the CCD detectors is stabilised at a temperature which is about 0.5 K cooler than that of the optical bench.

A layout of the OMI optical bench, depicting the telescope and the UV spectral channel, is presented in figure 1, where the large 114 degrees swath is out of the plane of the paper. The telescope consists of a primary mirror, a polarisation scrambler and a secondary mirror, focusing the incident radiance on the spectrograph slit 008. The telescope is f/15 in the flight direction and f/11 in the swath direction. The entrance aperture 001, which is only about 3 mm x 3 mm in area in order to suppress spatial stray light, does not limit the field or aperture. The polarisation scrambler makes the instrument insensitive to the polarisation of the incoming radiances, which simplifies the calibration of the instrument considerably. Note that the aluminium primary telescope mirror 003 is located before the polarisation scrambler, thus introducing a potential polarisation dependence of the instrument. However, the polarisation introduced by the primary telescope mirror is cancelled almost completely by the first surface of the polarisation scrambler. It has been verified by experiment that the polarisation dependence of the complete instrument to light parallel and perpendicular to the entrance slit is less than 0.5%. The secondary telescope mirror 007 has a coating that reduces the reflectance above 350 nm to about 40%. This, in combination with the selection of the various aperture sizes, has been done to accommodate the anticipated in flight radiance and irradiance levels and to optimise the performance of the scrambler. Solar irradiance enters the instrument through the solar port, which has a 10% transmission solar mesh, and illuminates one of three reflection diffusers (C04, C06, C06'). The solar port is closed by a shutter when not in use to protect the on-board diffusers. A folding mirror (C03) couples the diffuser signal into the main optical path just before the polarisation scrambler. The polarisation scrambler 005 consists of 4 wedged quartz plates. An on-board White

Light Source (WLS) is coupled in through a transmission diffuser C05 and the same folding mirror C03. For on-ground calibration purposes this optical path was also used by mounting external stimuli on a calibration port close to the WLS. The beam coming of either of the on-board diffusers illuminates the full length of the spectrograph slit and thereby all viewing directions (CCD rows) within the field-of-view. After the slit, in the spectrograph, the beam is split into two channels by dichroic mirror 009: the UV (270-380 nm) and the Visible (350-500 nm). The UV channel is separated into two sub-channels: UV1 (270-310 nm) and UV2 (300-380 nm), which decreases stray light at ultraviolet wavelengths and takes into account the significantly lower light fluxes from the earth below 300 nm as a result of ozone absorption. Mirror 104 is segmented and has a spatially grading efficiency coating that reduces reflectance of higher wavelengths at the lower part of the mirror to reduce stray light at the low wavelengths (below 310 nm). The UV1 channel is scaled down by a factor two in both dimensions, meaning that both the spectral and spatial sampling distances are 2 times larger as compared to the UV2 sub-channel. This has been done to improve the ratio between useful and dark signals in the UV1. The ratio between the spectral resolution and the sampling distance is about 3 in UV2 and VIS to avoid any difficulties caused by aliasing in the process of trace gas retrieval.

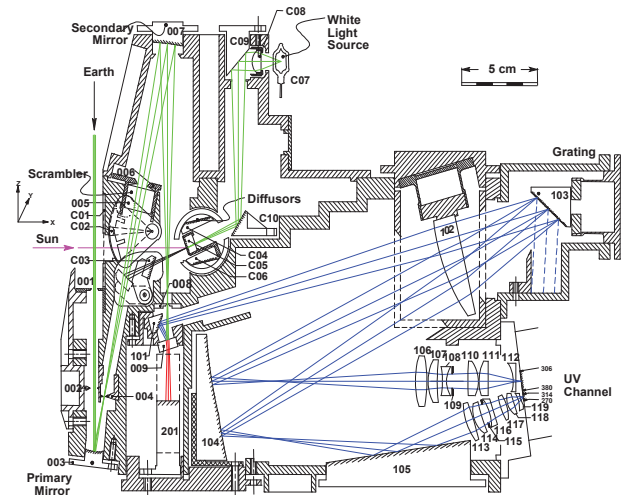


Fig. 1. Layout of the optical bench of the OMI instrument. Telescope + UV spectral channel. The light beam passing through dichroic mirror 009 is reflected by mirror 201 to the visible channel, which is not shown here.

The net integration time of 2 seconds, consisting of co-added 0.4 s individual exposures, sets the spatial sampling in the flight direction to 13 km. The CCD detector has a frame transfer layout to allow simultaneous exposure and readout of the previous exposure, avoiding data loss during readout. In the nominal operational mode (global mode) 8 CCD rows are electronically added (binned) during the readout, so spectra from neighboring viewing

directions are summed. This decreases the contribution of the readout noise and the internal data rate, and it increases the signal to noise. This sets the ground pixel size in the swath direction to 24 km.

The spatial and spectral properties of the OMI instrument are summarised in the table 1.

Table 1: spectral and spatial properties for the channels of the OMI instrument.

	Wavelength range (nm)	Sampling (nm/pixel)	Resol. (nm)	Pixel size (bin 8)
UV 1	270-310	0.32	0.65	13x48 km ²
UV 2	305-375	0.15	0.45	13x24 km ²
VIS	350-500	0.21	0.65	13x24 km ²

For in-flight calibration the OMI instrument is equipped with the following possibilities:

- A set of three reflective diffusers (C04, C06, C06') for absolute radiometric calibration by daily measurement of the sun. Two of the three diffusers are ground aluminium diffusers, one to be used on a weekly basis the other to be used monthly to monitor the degradation of the third diffuser. The third diffuser is a quartz volume diffuser that is used on a daily basis. This diffuser is ground on both sides and aluminium coated on the backside. The term volume diffuser refers to the fact that the first ground surface is used as a transmission diffuser, while the second aluminium coated surface acts as a reflectance diffuser. The first surface finally acts as a third transmission diffuser. The thickness of the diffuser is about 6 mm. These multiple diffusive surfaces reduce the effect of surface structures. The volume diffuser was implemented, because ground aluminium diffusers exhibit wavelength dependent interference structures that affect the accuracy of the radiometric calibration and that have a detrimental impact on the DOAS retrieval of data products. As a result of its smooth surface and the multiple diffusive surfaces the spectral structures introduced by the volume diffuser are at least an order of magnitude smaller. The diffusers are well protected from contamination and solar irradiance while not in use.
- The WLS C07 provides pixel-relative radiometric calibration and information about the degradation of the detector (bad/dead pixels). It can also be used to monitor the instrument radiometric calibration, albeit it with limited accuracy, because the lamp and its environment have not been designed to be radiometrically ultrastable.
- Two green LEDs per (sub)channel mounted in the proximity of the detector are also used to trace bad/dead pixels.
- At the eclipse side of the orbit the dark signal is calibrated by performing both long exposure time dark measurements and dark signal measurements

with instrument settings identical to radiance measurements at the dayside of the orbit.

- Spectral calibration is being performed using Fraunhofer lines in solar and nadir spectra. The OMI spectral slit function is known with high accuracy from the on-ground calibration. This precise knowledge of the slit function allows a wavelength calibration using a literature high-resolution solar spectrum and the observed spectrum.

3. RADIOMETRIC CALIBRATION

Past experience with satellite instruments similar to OMI (GOME, SCIAMACHY, TOMS, (S)SBUV) has shown that it is extremely important to obtain and measure any type of calibration parameter, but the radiometric calibration parameters in particular, under flight-representative thermal-vacuum pressure and temperature conditions. Outgassing of coated optical components and alignment changes over a 28 K temperature range (from room temperature 293 K to the operational temperature of 265 K) will introduce considerable changes that can not be reliably predicted in advance. For the on-ground calibration of the OMI instrument radiance earth mode and the irradiance sun mode are radiometrically calibrated in absolute sense under flight representative thermal vacuum pressure and temperature conditions (265 K) for the nominal viewing geometry. The viewing (swath) angle dependency of the absolute radiance and irradiance calibration parameters is necessarily measured under ambient environmental conditions. The radiance mode is dependent on the swath angle viewing direction of 114 degrees, while the irradiance mode depends on the solar elevation and azimuth angles. The elevation angle changes with satellite movement in orbit over a range -4.0 to +4.0 degrees with a nominal value of 0.0 degrees. The azimuth angle changes with season from 18 to 34 degrees with a nominal value of 26 degrees. The OMI instrument Bi-directional Scattering Distribution Function (BSDF) is measured under flight-representative environmental conditions. The BSDF is the key parameter to calibrate the absolute earth reflectance. The earth reflectance is the earth radiance divided by the solar irradiance, the basic input for all level 1-2 data product retrieval algorithms. The BSDF depends on swath angle, elevation and azimuth angles, diffuser, and of course wavelength.

As is seen in the optical layout presented in figure 1, the optical path for the radiance and the irradiance mode is identical except for the primary telescope mirror 003, that is unique for the radiance path, and the solar mesh, the on-board diffuser (C04, C06, C06') and the folding mirror C03, that are unique to the irradiance path. The other optical components in the OMI instrument are common for the (ir)radiance path and therefore cancel in first order in the ratio irradiance/radiance, which constitutes the instrument BSDF. Consequently the instrument BSDF includes the efficiency of the on-board diffuser, the solar

mesh, and the primary and the folding mirror. The aluminium on-board diffusers introduce spectral features in the irradiance signal. These features result from white light interference caused by the diffuser surface and they interfere with trace gas absorption structures in the earth reflectance spectrum and thereby hinder the retrieval of the column densities of these gases. To improve this a new type of quartz volume diffuser was developed that has much better spectral feature behaviour. As described in section 2, scattering by three surfaces effectively reduces interference effects. The absolute radiometric calibration, the BSDF calibration and the diffuser spectral features are treated in separate subsection below.

3.1 Absolute radiometric calibration

The absolute radiance calibration of the OMI instrument was performed employing 1000 Watts FEL QTH lamps, NIST traceable radiometric standards, and a calibrated 30x30 cm² spectralon diffuser panel. The absolute irradiance calibration was derived by combining the absolute radiance calibration and the OMI instrument BSDF, that is discussed in the next section. The FEL lamp illuminates the spectralon diffuser panel perpendicularly at a 50.0 cm distance. The OMI instrument was residing in a thermal vacuum chamber at stable flight representative vacuum pressure and temperature conditions. Appropriate measures were taken to prevent stray light reflections from the interior walls of the vacuum chamber. A viewing angle of 40 degrees on the diffuser panel was employed. In the employed setup for absolute radiance calibration only a small part (~4 degrees) of the 114 degree large field-of-view of the OMI instrument was illuminated instantaneously and, as a result of the fact that it was not possible to rotate the OMI instrument in the thermal vacuum chamber, the absolute radiance calibration at flight representative thermal vacuum temperature and pressure conditions is only available for nadir zero viewing angle. The viewing angle dependence of the absolute radiance sensitivity of the OMI instrument for off nadir viewing angles is derived from ambient measurements, where the instrument was rotated on a turn-tilt cradle. It is questionable whether the radiance swath angle dependency is the same for ambient and for flight-representative thermal-vacuum conditions. The swath angle dependency of the radiance calibration will be the subject of detailed investigation in flight. The elevation and azimuth angle dependency of the absolute irradiance calibration was also measured under ambient environmental conditions and combined with the absolute irradiance calibration at the nominal angles, which was measured under thermal-vacuum conditions in the vacuum chamber. The irradiance goniometry will also need to be investigated in flight.

The absolute radiance sensitivity of the OMI instrument at flight representative thermal vacuum conditions for nadir zero viewing angle is shown in figure 2. The enhanced sensitivity of the UV1 spectral channel, that is achieved

by scaling down the channel both in the spectral and in the spatial dimension, is clearly visible in the plot.

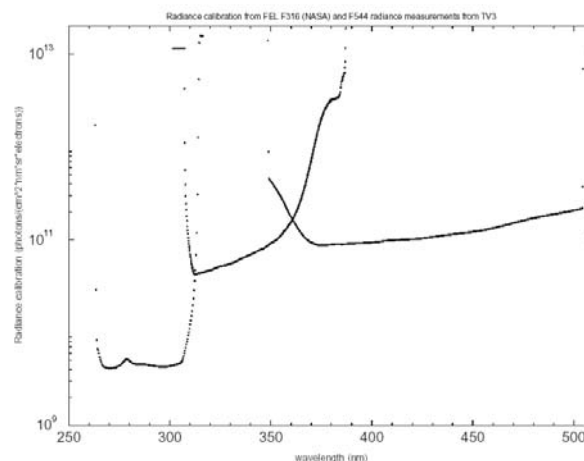


Fig. 2. The absolute radiance calibration of the OMI instrument for nadir zero viewing direction, measured at flight representative thermal vacuum pressure and temperature environmental conditions. The enhanced sensitivity in the UV1 spectral channel results from scaling down the channel by a factor two in both the spectral and the spatial dimension. The optical channel boundaries are at about 305 and 370 nm.

3.2 BSDF calibration

The BSDF of the OMI instrument was calibrated using a dedicated optical stimulus with a divergence of at most 0.5 degree (depending on wavelength), similar to the sun, and an output beam with a diameter of about 8 cm. The optical design guarantees an unpolarised output beam with a rest polarisation <1%. The light source of the stimulus is an ultrastable 100 Watts xenon plasma source, ensuring long-term stability during and between the radiance and irradiance measurements. Spatial uniformity of the stimulus is very important for the BSDF measurements. During the BSDF measurements the instrument was at stable flight representative thermal vacuum conditions. For deriving the absolute value of the OMI instrument BSDF the thermal vacuum measurements for nadir zero degrees viewing direction are used. The viewing angle dependency of the OMI instrument BSDF is necessarily measured in ambient, because a turn-tilt cradle to rotate the OMI instrument in the thermal vacuum chamber was not available. The viewing angle dependency of the OMI instrument BSDF was also measured at one off-nadir measurement (+50 degree viewing direction) at flight representative thermal vacuum conditions, but this result did not produce the same swath angle dependency as obtained for the ambient conditions. The comparison is also hampered by the reduced signal-to-noise of the ambient measurements as a result of the reduced detector performance at ambient conditions. This implies that the swath angle dependency of the BSDF will have to be verified carefully in flight.

The OMI instrument BSDF for nadir zero degrees measured at flight representative thermal vacuum conditions is presented in figure 3 for all three on-board diffusers. The BSDF curve for the quartz volume diffuser is approximately a factor two lower than the BSDF curves for the two aluminium diffusers, as a result of the lower reflectivity efficiency of the quartz volume diffuser. A wavelength dependent BSDF difference between both aluminium diffusers of up to 15% is measured. The spectral structure in the BSDF of the aluminium diffusers above 400 nm originates from the spectral diffuser features.

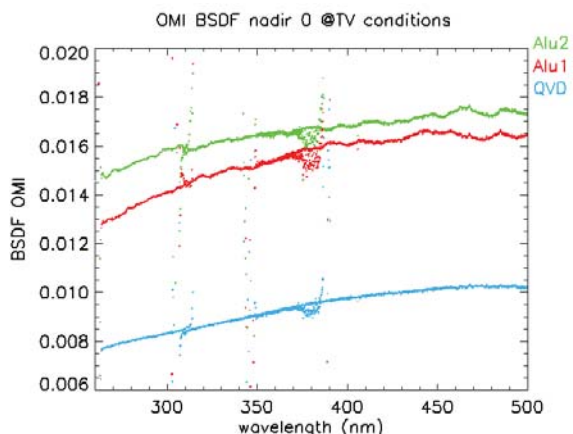


Fig. 3. OMI instrument BSDF for nadir zero degrees viewing angle measured at thermal vacuum environmental conditions for all three on-board reflection diffusers.

3.3 Diffuser features in the irradiance

Aluminium reflection diffusers introduce spectral structures in the irradiance signal and consequently in the earth reflectance spectrum. These spectral features have been shown to result from white light interference effects from the diffuser surface. The BSDF curves for the aluminium on-board diffusers presented in figure 3 clearly exhibit diffuser spectral features. When the periods and amplitudes of these spectral features are comparable to trace gas absorption features they interfere with DOAS-based retrieval of trace gases, affecting the accuracy of the retrieved column densities. For this reason the quartz volume diffuser, which exhibits much smaller amplitude spectral features, was developed and integrated into the instrument. The diffuser spectral features are clearly visible in the ratio of spectra taken at different illumination angles (azimuth and/or elevation), and their amplitude and behaviour, e.g. rapid or slow variations with changing azimuth/elevation angle, can be studied this way. However, the features in the ratioed irradiance measurements are not identical to the features as they show up in the earth reflectance spectrum. A limited measurement program was performed in ambient environmental conditions to assess the behaviour of the spectral features at a rather coarse grid. Figure 4 shows the ratio of a single elevation measurement over the average of all elevation angles in the range -3.0 to $+3.0$

degrees for the quartz volume diffuser (top) and for the aluminium diffuser (bottom) for 310-500 nm wavelength range. The amplitude of the spectral features for the aluminium diffuser is 5-10% peak-peak, whereas the feature size for the quartz volume diffuser is at least one order of magnitude smaller. A 5% feature size would be very unfavourable to DOAS retrievals, as the size of absorption features of trace gases typically measure 10^{-3} - 10^{-4} . Apart from affecting the DOAS retrieval the spectral features also influence the accuracy of the level 1 irradiance product. A full characterisation and calibration of the diffuser spectral features will have to be performed in-flight using irradiance measurements, because the exact same illumination conditions can not be reproduced on the ground. For example, differences in beam divergence lead to different detailed appearances of the spectral diffuser features, although the overall behaviour remains the same. Furthermore, the on-ground ambient measurements suffered from reduced signal-to-noise as a result of the reduced detector performance at ambient conditions (higher dark current and more noise). Possible algorithms to reduce the impact of both the aluminium and quartz volume diffuser spectral features include averaging spectra obtained at various elevation angles (these are

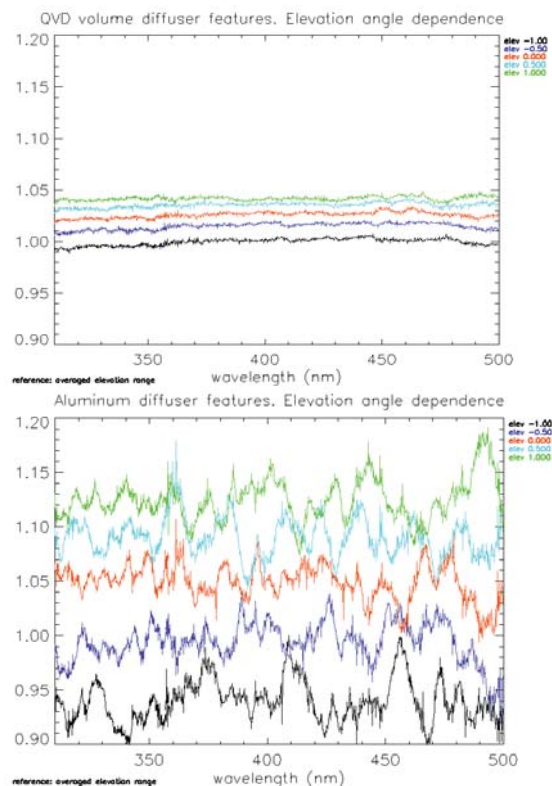


Fig. 4. Ratio of single elevation angle measurement over the average of all elevation angles in the range $[-3.0, +3.0]$ degrees for the quartz volume diffuser (top) and the aluminium diffuser (bottom) for the 310-500 nm wavelength range.

obtained in one solar observation sequence as a result of the satellite movement) and binning of CCD detector rows over 8 or more rows.

Beside spectral features the aluminium diffusers also exhibit spectrally independent features, with amplitudes in the order of several percent, that manifest themselves in the spatial (row) direction of the irradiance illumination profile. These high frequent features, which show almost no wavelength dependence, are caused by randomly distributed specularly reflective spots on the ground surface of the aluminium diffuser. The pattern of these wavelength independent features varies strongly with illumination angle. The occurrence of these features affects the viewing angle dependency calibration accuracy of the OMI instrument BSDF. One of the reasons for the diffuser features to show up so profoundly is that a CCD detector pixel only views a small area of the on-board diffuser (about 2 mm²), because the on-board diffusers are located close to the focus of the telescope. This renders the pixel-signal sensitive to local wavelength (in)dependent variations of diffuser reflectivity, rather than averaging them out as would be the case when a detector pixel would view a much larger area of the on-board diffuser. The row-dependent features are virtually absent for the quartz volume diffuser.

4. SPECTRAL CALIBRATION AND SPECTRAL SLIT FUNCTION CALIBRATION

The calibration of the spectral properties of the OMI instrument comprises two aspects: the spectral assignment and the shape of the spectral response function (slit function) of each detector pixel. Both calibration parameters were measured with the OMI instrument at flight-representative thermal vacuum pressure and temperature environmental conditions.

The spectral response, or slit function, determines how spectral structures in the input (ir)radiance are smeared and recorded by the OMI instrument. This is of great importance for DOAS based retrieval of data products where the structures in the observed earth reflectance spectrum are fitted by an accurate spectrum of the trace gas of interest smeared to OMI resolution in order to retrieve its column density. For the purpose of accurately measuring the slit function shape a dedicated optical stimulus was designed that utilises an echelle grating to produce an output beam containing ~50 tunable, well separated, narrow spectral peaks (diffraction orders) in the OMI wavelength range. By turning the echelle grating the peak positions in the stimulus output beam move in wavelength space. The response of a detector pixel to a passing echelle peak constitutes the spectral slit function of that pixel. Thus, the number of sampling points on the measured slit function is determined by the number of rotation steps of the echelle grating, which can be chosen freely. By employing this method the shape of the spectral slit function is measured with better sampling, and at higher accuracy, than is obtained using a spectral line

source, in which case the accuracy is limited by the sampling of the spectral resolution by the detector. As listed in table 1 the ratio spectral resolution/sampling of the OMI instrument is typically 3, whereas in the dedicated slit function measurements a ten times better sampling of the spectral resolution is easily achieved (note that the factor of ten is no limitation, but can be chosen freely by selecting the echelle grating rotation steps). The light beam of the stimulus was coupled into the OMI instrument using the calibration port, which was described in section 2. In this way the full length of the spectrograph slit and thereby all CCD-rows (viewing angles) were illuminated instantaneously, enabling the slit function profile of all CCD pixels to be measured in a single measurement run. Figure 5 shows in the upper plot the sampling of the spectral slit function when recording the response to a spectral line source while the lower plot shows the improved sampling of the slit function measured using the dedicated echelle grating optical stimulus. The solid line is a functional fit through the data points of the lower plot. The fit result is co-plotted in the upper panel for comparison. For the UV1 spectral channel a regular Gaussian line shape was fitted, for the UV2 and VIS spectral channels a modified, broadened Gaussian profile was used. The functional describing the broadened Gaussian profile is given in the following equation:

$$A_0 e^{-\left(\frac{x-x_0}{w_0}\right)^2} + A_1 e^{-\left(\frac{x-x_1}{w_1}\right)^4} \quad (1)$$

with A_0 , A_1 , x_0 , x_1 , w_0 , w_1 being fitting parameters. Note that x_0 and x_1 can be different, resulting in asymmetric slit function shapes.

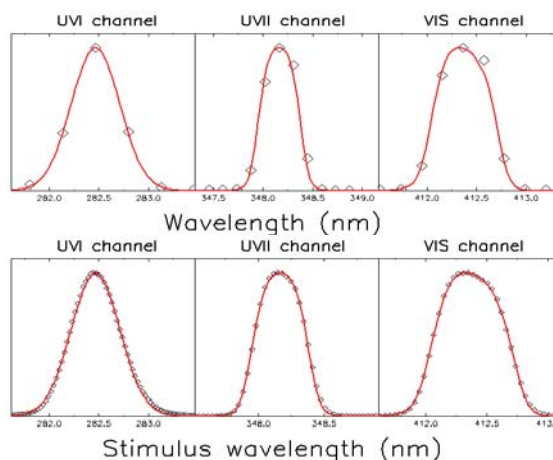


Fig. 5. The OMI spectral slit function profile for each spectral channel. The upper panel presents the OMI response to a spectral line, the limited sampling of OMI's spectral resolution is clearly visible. The lower panel presents the OMI slit function calibrated with the dedicated optical stimulus; much higher sampling is achieved with this stimulus. The solid line is a functional fit through the data, a Gaussian profile in UV1, a modified (broadened) Gaussian profile in UV2 and VIS. The fit

result of the lower panel is co-plotted in the upper panel for comparison.

The spectral calibration was performed using a hollow cathode PtCrNe spectral line source. However, this light source suffers from a number of disadvantages. Firstly, this line source lacks sufficiently strong lines in the high end of the OMI wavelength range (above 450 nm). Secondly, the spectral lines are often blended at the OMI spectral resolution, which makes peak fitting and determination of the peak maxima less accurate than for single unblended lines. Thirdly, the instrumental sampling in the wavelength dimension is obtained by about 5 points per spectral line. These few points must then be used to determine the slit function and the peak maximum, but with so few points it is difficult to get a sufficiently accurate result. Furthermore, for some wavelength regions no or only weak spectral lines are available. It is difficult to obtain an accurate slit function calibration or information for the spectral calibration from such weak lines. Finally, the distribution of the spectral lines results in some wavelength ranges where no or only a small number of spectral lines are available. This results in incomplete and uneven coverage and distribution of the lines over the optical channels. For these reasons the hollow cathode lamp measurements were combined with the slit function measurement data obtained with the echelle optical stimulus to derive a much more accurate wavelength calibration, yielding an on-ground wavelength calibration accuracy of 1/10 pixel (~0.01 nm). Combining the hollow cathode lamp measurements with known literature atomic emission lines with the echelle optical stimulus measurements is required, because the latter optical stimulus does not have an absolute wavelength scale. The final accuracy obtained by this method is sufficient for the wavelength assignment of the other on-ground calibration measurement data (e.g. radiometric calibration data). It was also successfully verified that the spectral calibration and the slit function calibration are identical for all three of the OMI optical entrance ports: nadir port, solar port and the calibration port, which was only used during the on-ground calibration phase.

For the in-orbit wavelength calibration a high-resolution solar spectrum convolved with the calibrated slit function will be used. This spectrum is compared with the solar measurement in order to determine the spectral calibration and verify the spectral slit function. Using the Fraunhofer structures in the solar spectrum the required accuracy for the in-flight wavelength calibration of 1/100 pixel is expected to be met.

5. IN-FLIGHT CALIBRATION

In-flight calibration and trend monitoring of the instrument is essential to maintain a good calibration status of the instrument, for which the on-ground calibration is the starting point, and to investigate the behaviour of the instrument under flight representative conditions. These conditions not only include pressure and

temperature, but also illumination conditions in terms of intensity, stray light, divergence and polarisation. As a result of ultraviolet illumination, contamination and particle flux, or a combination thereof, the efficiency throughput of the instrument may degrade optically, electronically and for the CCD detectors. All possible precautions have been taken to minimise the impact of these effects. Aluminium shielding has been applied in the instrument design to protect against high-energetic particles in space. Optical components are stowed away when not in use (diffusers, folding mirror). Immediately after launch the instrument is outgassed at 298 K for four weeks in order to get rid of as much contaminants as possible. The diffusers are not used before seven weeks after launch in order to ensure that no contaminants burn onto the surfaces in combination with ultraviolet irradiation. But despite these precautions it is to be expected from previous missions with similar instruments (TOMS, SBUV, GOME, SCIAMACHY) that the OMI instrument will show a certain extent of throughput degradation, which can not be predicted in advance and which may very well be irregular. In addition, some parameters can not be reliably calibrated on the ground, because the exact same illumination conditions can not be reproduced. An example are the on-board diffuser features, discussed in detail in section 3.3. For all these reasons a good in-flight calibration is essential.

For OMI the in-flight calibration concept is deeply embedded into the operation concept: of the total of 66 operational instrument configurations that are used, 57 configurations serve the purpose of in-flight calibration. The calibration measurements are based on earth, sun, WLS, LED and dark measurements. Parameters that are varied include diffuser, exposure time, binning factor, gain factors. During the Launch and Early Operations Phase even more dedicated calibration configurations are used. By combining these measurements it is possible to a certain extent to identify which component is changing or degrading and quantify these changes. For OMI the algorithms to do this are described in detail in the in-flight calibration plan. This information must then be fed back into the data processing system to correct for the changes. The 0-1 data processor ingests raw level 0 instrument data and produces three output products: a radiance product, an irradiance product and a calibration product. All three can in principle be used for in-flight calibration and trend monitoring, but the irradiance and the calibration products are routinely used in the automated system. The 0-1 data processor uses the so-called Operational Parameter File (OPF), which contains all relevant instrument calibration and characterisation data required to transfer pixels and binary units into wavelengths, viewing angles, and radiances or irradiances. The OPF size is typically 100 MBytes. The 0-1 data processor contains all necessary algorithms to perform the electronic, detector, radiometric, geometry and stray light correction steps. Before launch the 0-1 data processor and OPF are planned to be extensively tested in a closed-loop system, with

measurement data from known light input scenario's to the instrument. The output of the 0-1 data processor can then be compared to the known inputs to the instrument. Per orbit of 100 minutes about 150 MBytes of calibration data is generated. With these amounts of data of data a fully automated data processing system is required in order to keep up with the incoming data. The data arrives at the Trend Monitoring and Calibration Facility (TMCF), which is part of the OMI Dutch Processing System (ODPS) at KNMI in De Bilt, The Netherlands. The 0-1 data processor is running in the Science Investigator-led Processing System (SIPS) at Goddard Space Flight Center (GSFC) in Washington D.C., U.S.A. The orbit data is ingested in the TMCF and split according to measurement type and measurement configuration. This step creates new data products within the TMCF. Subsequently, data configurations of the same type are averaged automatically, using predefined production rules to start Product Generation Executables (PGE's). PGE's are pieces of software that perform the requested tasks. When the required data is available, orbital, daily, weekly and monthly averages are automatically created as well as stored as data products. The next automated step invokes more PGE's that operate on the measured or averaged data and perform more detailed in-flight calibration and trend monitoring analysis tasks. For example, PGE's exist that calculate the detector pixel response non-uniformity (PRNU), electronic gain ratio's, linearity, dark current, bad and dead pixels, instrument degradation from the solar measurements, instrument degradation from the WLS measurements and LED measurements, etc. All these PGE's use specific input data products within the TMCF that are created by the preceding automated steps. The PGE's produce dedicated output products, that are also stored. All data that is ingested in the TMCF, the output of the measurement configuration split process, the output of the average process and the output of the analysis PGE's are stored in the so-called in-flight calibration and trend monitoring database, which is also part of the TMCF. This database retains most products originating from calibration and irradiance data products for the duration of the whole mission. All data ingested in the ODPS and TMCF is also stored on a tape system. However, some of the very frequent dark signal measurements are regularly erased from the database after some time, e.g. three months, in order to keep the database size within reasonable limits. The averaged data are always kept in these cases. The MySQL-based database, which is stored on the hard disks of the TMCF for fast access, can grow to several TBytes after five years, the anticipated duration of the mission. All stored data is in HDF-EOS 2.7 (HDF 4) format.

Besides the automatic processing it is also possible to start PGE's manually. In these cases the production rules have to be generated manually in advance as well. PGE's of this type include more complex in-flight calibration algorithms, such as CCD detector pixels random telegraph effect identification, which requires data sets that may

cover more than one month, spectral and spatial stray light and geolocation calibration or verification. Thus, the PGE's running in the TMCF fill the in-flight calibration and trend monitoring database. Using these data new OPF parameters can be generated automatically, which can subsequently be used by the 0-1 data processing system. In this way the most accurate calibration of the instrument is used for data processing. It is too risky to run this loop fully automated without human control. For this reason an in-flight calibration specialist regularly sends the automatically updated OPF's to the GSFC data processing site, e.g. once per month. All OPF's as a function of time describe the time-dependent long term degradation behaviour of the instrument. In order to interpolate and extrapolate between various OPF's the following mechanism has been developed: Once per week an automatically generated new OPF with the most actual instrument data is transferred to the GSFC 0-1 data processing site after having been tested for completeness and quality. This OPF also contains the time behaviour of the time-dependent parameters. An OPF preprocessor, which still needs to be developed, uses this one OPF to generate an OPF for each orbit, as a preprocessing step to the 0-1 data processor. In this way the most accurate OPF, including the time-dependent behaviour, is always used in the 0-1 data processing system. The time dependence of the new OPF also contains the predictions for the future, until another new OPF is provided.

6. CONCLUSIONS

The OMI mission on the EOS-AURA satellite, to be launched in the second half of 2004, was discussed and the instrument properties and design were described in detail. Results from the radiometric calibration (radiance, irradiance and instrument BSDF) were shown and discussed. The results show that the angle dependencies of the radiance and irradiance need further attention in flight. The radiometric instrument BSDF and irradiance calibrations were shown to be influenced by both wavelength-dependent and wavelength-independent features from the on-board aluminium diffusers. Both types of features depend on the viewing direction (swath angle). These diffuser features need further attention in flight as well. The quartz volume diffuser, which will be used daily, is comparatively unaffected by these diffuser features.

A new technique, based on an echelle grating optical stimulus, was used for OMI to calibrate the spectral slit functions and derive an accurate spectral calibration. The results show that with this new method the spectral calibration and the spectral slit function calibration are considerably more accurate than with techniques that were used previously.

The in-flight calibration approach and systems were discussed. These systems will be available and ready at launch to support the in-flight calibration and long term trend monitoring.